coatings

MDPI

Article

Precision Machining of Nimonic C 263 Super AlloyUsing WEDM

Katerina Mouralova [1], Libor Benes [2], Josef Bednar [1,*], Radim Zahradnicek [3], Tomas Prokes [1], Zdenek Fiala [4] and Jiri Fries [5]

1 Faculty of Mechanical Engineering, Brno University of Technology, 616 69 Brno, Czech Republic; mouralova@fme.vutbr.cz (K.M.); tomas.prokes@vutbr.cz (T.P.)
2 Faculty of Production Technologies and Management, Jan Evangelista Purkyně University, 400 96 Ústí nad Labem, Czech Republic; libor.benes@ujep.cz
3 Faculty of Electrical Engineering and Communication, Brno University of Technology, 616 69 Brno, Czech Republic; zahradnicek@vutbr.cz
4 INTEMAC Solutions Ltd., 664 34 Kurim, Czech Republic; fiala@intemac.cz
5 Department of Production Machines and Design, Technical University of Ostrava, 708 33 Ostrava, Czech Republic; jiri.fries@vsb.cz
* Correspondence: bednar@fme.vutbr.cz

Received: 30 May 2020; Accepted: 22 June 2020; Published: 24 June 2020

Abstract: Wire electrical discharge machining (WEDM) is an unconventional and very efficient technology for precision machining of the Nimonic C 263 super alloy, which is very widespread, especially in the energy, aerospace and automotive industries. Due to electrical discharge, defects in the form of cracks or burned cavities often occur on the machined surfaces, which negatively affect the correct functionality and service life of the manufactured components. To increase the efficiency of the machining of Nimonic C 263 using WEDM, in this study, extensive design of experiments was carried out, monitoring input factors in the form of machine parameters like Pulse off time, Gap voltage, Discharge current, Pulse on time and Wire feed, the output of which was comprehensive information about the behaviour of such machined surfaces, which allowed the optimization of the entire machining process. Thus, the optimization of the Cutting speed was performed in relation to the quality of the machined surface and the machining accuracy, as well as an analysis of the chemical composition of the machined surfaces and a detailed analysis of the lamella using a transmission electron microscope. A detailed study of the occurrence of surface or subsurface defects was also included. It was found that with the help of complex optimization tools, it is possible to significantly increase the efficiency of the machining of the Nimonic C 263 super alloy and achieve both financial savings in the form of shortened machine time and increasing the quality of machined surfaces.

Keywords: WEDM; wire electrical discharge machining; nimonic; design of experiment; machining parameters

1. Introduction

Wire electrical discharge machining (WEDM) technology, one of the most unconventional machining technologies, has been indispensable in many areas of industry for more than 50 years. It plays a key role mainly in the automotive, aerospace, energy and military industries, despite its higher energy intensity. Due to the fact that the removal of material is realized in a non-contact manner by means of periodically repeating electric discharges between the electrode and the workpiece, no classical forces affect the material and thus do not deform it. It is, therefore, possible to machine all at least minimally electrically conductive materials without taking into account the set of their physical

and mechanical properties, such as hardness or toughness. It is thus possible to machine materials after final heat treatment or to produce thin-walled profiles even for very soft or very tough materials [1,2].

Due to the fact that the only condition for successful machining is electrical conductivity, WEDM technology is popularly used for newly discovered composite materials or highly tough aviation alloys, which are difficult to machine using conventional technologies. Another advantage is that there is no need to wait for tool manufacturers to develop a tool for conventional machining of these difficult-to-machine new materials. The tool during WEDM is always a wire with a diameter of 0.03 to 0.3 mm, which is most often made of brass, while other types of wires are copper or coated or composite [3,4].

Conventional machining of Nimonic C-263 has always been a challenging task owing to its low thermal conductivity, heat strength, affinity towards tool materials and tendency to undergo work hardening. For these reasons, wire electrical discharge machining technology has proven to be the most suitable method for machining this super alloy [5].

WEDM technology is a key machining process; however, thanks to its increased energy consumption, there is an effort to minimize this cost item as much as possible, especially by reducing machine time. The machining length in the form of cutting speed can be reduced primarily by the suitable optimization of the machine parameters settings, while also taking into account the resulting quality of the machined surface and also the dimensional accuracy. To optimize the WEDM process for different materials, many extensivedesigns of experiments and studies have been performed, e.g., optimizing the machining of Creusabro [6], Hardox [7] or Hadfield steels [8] and aluminium alloys 7475-T7351 [9], or finding the occurrence of subsurface defects depending on their lifetime [10]. The aim of this study was to present the results of a detailed and extensive optimization process for machining the Nimonic C 263 super alloy using WEDM, and no such extensive experiment has been performed with this material in similar studies. However, the complex investigation of the effects of WEDM on this widely used material is absolutely crucial in order to achieve its efficient machining. Nimonic alloys are indispensable in many industries, including the aerospace, automotive and energy industries, with the Nimonic C 263 typically being used in the hot combustion portion of gas turbines.

Literature Review

Goswami [11] examined the surface integrity, wire wear ratio and MRR during the WEDM process. As an experimental material, Nimonic 80A alloy was used. To plan and design the experiments, the Taguchi method was employed. In the main outputs of the research, it was pointed out that a higher value of the Pulse on time causes a thicker recast layer. On the contrary, a lower value of Pulse on time but a higher value of Pulse off time causes low wire deposition on the surface being machined. Mandal [12] focused on the machining of Nimonic C-263 super alloy, which is characterized by tool wear rate and high hardness. Thus, he investigated the impact of WEDM parameters on various important performance measures during machining. Consequently, a mathematical model was developed, and the responses were employed to investigate the interrelationship between the process parameters and performance measures. Mandal [13] studied the surface integrity improvement of Nimonic C 263 super alloy, while the WEDM process was employed with different post-processing techniques, for example, etching-grinding and grinding, explaining their basic mechanisms. This proved to be very effective and efficient for complete recast layer removal and surface generation. Amitesh [14] focused in their research on the machining characteristics of the material Nimonic 80A during the WEDM process and studied the dependency of machining parameters employed in the experiments on the material removal rate and cutting speed. It was discovered that two parameters (Pulse on time and peak current) increase the MRR and CS while being increased themselves, and the other two parameters (Pulse off time and spark gap set voltage) decrease them while being increased. Bisaria [15] also investigated the material of Nimonic C-263 super alloy during the WEDM process. A one-parameter-at-a-time approach was employed in the experiments to study the effect of the machining parameters on the investigated material. They focused their attention on the surface morphology and topography,

recast layer thickness and surface roughness among the others. Sonawane [16] focused on the machining parameters optimization during the WEDM process and studied Nimonic-75 as a material for the experiments. In their research, they employed principal component analysis, which they combined with the Taguchi method. The parameter of Pulse on time turned out to be the most effective factor influencing the performance characteristics. Goswami [17] also tried to investigate the optimal machining parameters for the electrical discharge machining of Nimonic-80A alloy. In their experiments, however, they integrated the Taguchi approach and the utility concept with a multi-response optimization method. The main focus of their research was the following machining characteristics as the surface roughness and material removal rate and their interactions with the studied parameters. Kumar [18] investigated the WEDM process and the parameters while machining Niminic-90, i.e., a nickel-based aerospace alloy. The parameters studied were modelled for the main response variables, such as surface roughness, cutting speed and radial overcut, where the quadratic model was used. The response surface methodology was also employed for the investigation of the machining parameters. Singh [19] studied the machining process of Nimonic 263 material during the WEDM process, trying to create an empirical model of wear ratio that was best suited for prediction. They also studied how the process parameters affect the machining process. The experiments showed that the input process parameters have a great impact on process performance characteristics.

2. Experimental Setup and Material

2.1. Experimental Material

The samples for the experiment shown in Figure 1a were made of nickel super alloy Nimonic C 263 with chemical composition according to the standard in weight percent 20% Cr, 16.7% Co, 6.3% Mo, 0.45% Mn, 1% Fe, 1.9% Ti, 0.5% Al, 0.04% Nb, 0.15% W, 0.07% Cu, 0.19% Si, 0.02% V, 0.02% C, 0.001% S, 0.007% Ta, Ni-balance. The microstructure shown in Figure 1b clearly reveals the presence of hard and abrasive carbide particles such as $(Cr,Mo)_{23}C_6$ along with preferential segregation distributed in the grain boundaries [20]. Nimonic C 263 has a hardness of 300 HV, a yield strength of 400 MPa, a tensile strength of 540 MPa, and a creep strength of 120 MPa. It is most often used for the production of turbine blades, springs resistant to high temperatures, components of industrial furnaces or as a mounting material for aerospace. An initial semi-product with a thickness of 7 mm was used for the experiment, the length of the section of each sample always being 3 mm.

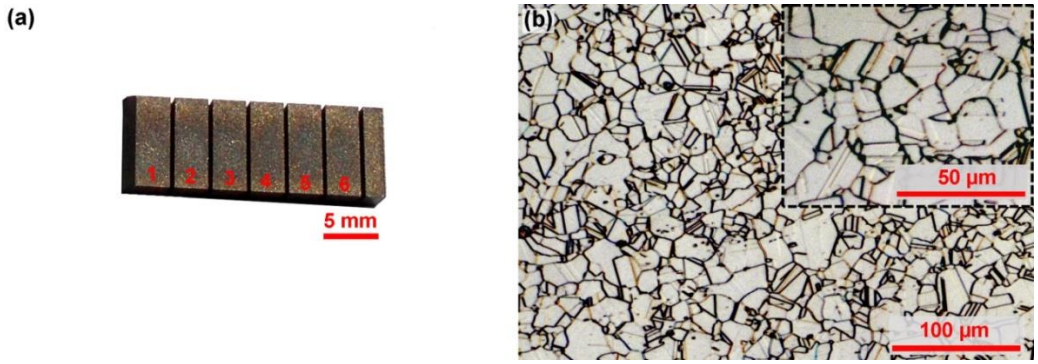

Figure 1. (**a**) example of produced samples during the experiment, (**b**) microstructure of Nimonic C-263 material.

2.2. WEDM Machine Setup

A five-axis EU64 EDM wire cutter from the manufacturer MAKINO was used for machining, which is equipped with CNC control and also an impregnation bath, in which the workpiece is completely immersed throughout the machining. Deionized water was used as the dielectric, which allowed highly efficient cooling and flushing of eroded material particles from the cutting place. The tool electrode was a brass wire (60% of Cu and 40% of Zn) of the CUT E type from the manufacturer PENTA with a diameter of 0.25 mm.

A design of experiments (DoE) is a test or multiple tests in which the input parameters of a process are systematically changed in order to determine the corresponding changes in the output variable, the so-called response. The response is modelled using regression analysis and analysis of variance (ANOVA). With DoE, the significance of predictors and their settings can be determined, allowing the process to be optimized. The design of experiments performed in this study was based on monitoring the influence of five independent machine setup parameters: Pulse off time (T_{off}), Gap voltage(U), Discharge current(I), Pulse on time (T_{on}), Wire feed(v) and their limit values as written in Table 1. The limit values for setting the individual parameters have been determined on the basis of extensive previous tests [21].

Table 1. Values of machine setting parameters.

Parameter	Gap Voltage (V)	Pulse onTime (µs)	Pulse off Time (µs)	Wire Feed ($m \cdot min^{-1}$)	Discharge Current (A)
Level 1	50	6	50	10	25
Level 2	60	8	40	12	30
Level 3	70	10	30	14	35

The "Central composite response surface design", containing 33 rounds divided into two blocks, was chosen for the experiment, as recorded in Table 2. This design is a composition of "Half factorial design 2^{5-1}" and 10 axial points. To better statistically estimate the variability of the response, the experiment was supplemented by seven central points, and to reduce the possibility of systematic errors, the individual rounds were randomized. This data collection plan is described in detail, for example, in Montgomery [22]. Furthermore, Table 2 shows the response of the machining process, which was the Cutting speed v_c. This was read directly from the machine display during the machining of each of the samples.

Table 2. Parameters used in the experiment and Cutting speed.

Number of Sample	Gap voltage (V)	Pulse on Time (μs)	Pulse off Time (μs)	Wire Feed ($m \cdot min^{-1}$)	Discharge Current (A)	Cutting speed ($mm \cdot min^{-1}$)	Number of Sample	Gap voltage (V)	Pulse on Time (μs)	Pulse off Time (μs)	Wire Feed ($m \cdot min^{-1}$)	Discharge Current (A)	Cutting Speed ($mm \cdot min^{-1}$)
1	70	8	40	12	30	3.4	18	60	8	40	12	30	3.4
2	60	8	30	12	30	3.6	19	60	8	40	12	30	3.4
3	60	8	40	12	25	2.95	20	70	6	50	14	25	2.35
4	60	10	40	12	30	3.9	21	50	6	30	14	25	3
5	50	8	40	12	30	3.3	22	60	8	40	12	30	3.4
6	60	8	50	12	30	3	23	70	10	30	14	25	3.3
7	60	6	40	12	30	3	24	50	6	50	10	25	2.4
8	60	8	40	12	35	3.85	25	60	8	40	12	30	3.4
9	60	8	40	10	30	3.4	26	50	10	50	14	25	2.9
10	60	8	40	14	30	3.35	27	50	10	30	10	25	3.5
11	60	8	40	12	30	3.4	28	50	6	50	14	35	3
12	50	6	30	10	35	3.7	29	50	10	50	10	35	4
13	70	10	50	10	25	2.9	30	70	6	30	14	35	3.6
14	70	10	30	10	35	4.1	31	50	10	30	14	35	4
15	60	8	40	12	30	3.4	32	60	8	40	12	30	3.4
16	70	6	50	10	35	3	33	70	6	30	10	25	3.2
17	70	10	50	14	35	3.75							3.4

3. Results and Discussion

3.1. Experimental Methods

All experimentally produced samples were cleaned in an ultrasonic cleaner and analysed using an LYRA3 electron scanning microscope (SEM) from Tescan. This device was equipped with an energy-dispersive X-ray detector (EDX), which allowed the study of the change in the chemical composition of the surface of the cut material due to the WEDM machining. For the analysis of surface and subsurface microstructural changes and the measurement of the cut gap, metallographic sections of cross-sections were prepared from the machined material by the WEDM method. These samples were prepared by conventional techniques—wet grinding and diamond paste polishing using the Struers TEGRAMIN 30 automatic preparation system. The final mechanical-chemical finishing was performed using a Struers OP-Chem suspension. After etching with Kalling's etch 2, the structure of the material was observed and documented by electron and light microscopy on an inverted light microscope (LM)Axio Observer Z1m from ZEISS. The topography and 3D reliefs of surfaces were studied using a Dektak XT 3D contact profilometer supplied by Bruker. The measured data were then processed in Vision 64 and Gwyddion software. Using a focused intense beam (FIB) on a Helios microscope from FEI, a lamella was prepared to study the material composition using EDX in a transmission electron microscope (TEM) Titan from FEI.

3.2. Statistical Evaluation of Cutting Speed

The Cutting speed of individual samples was read from the machine display during machining and written to Table 3., from which it is evident that the Cutting speed ranged from 2.35 to 4.1 mm·min^{-1}. The highest speed was achieved with the set of parameters for Sample 14, namely U = 70 V, T_{on} = 10 µs, T_{off} = 30 µs, v = 10 m·min^{-1} and I = 35 A. The Cutting speed of all samples in this study was significantly higher than when machining in the Mandal study [12], which may be due to half of the thickness of the material being machined.

Table 3. Variance of Cutting speed.

Cutting Speed (mm/min)	Contribution	Effect	*p*-Value
Model	97.30%		0
Linear	91.89%		0
Pulse on time (µs)	26.19%	0.5667	0
Pulse off time (µs)	22.24%	−0.5222	0
Wire speed (m/min	0.91%	−0.1056	0.009
Discharge current (A)	42.54%	0.7222	0
Square	1.55%		0.001
Pulse off time (µs)*Pulse offtime(µs)	1.55%	−0.2044	0.001
2-Way Interaction	3.86%		0
Pulse on time (µs)*Pulse off time (µs)	2.22%	0.1750	0
Pulse on time (µs)*Discharge current (A)	0.92%	0.1125	0.009
Pulse off time (µs)*Discharge current (A)	0.72%	0.1000	0.018
Error	2.70%		
Lack-of-Fit	2.70%		Impossible to determine
Pure Error	0.00%		
Total	100.00%		

* Multiplication symbol.

A full quadratic regression model including "Analysis of Variance (ANOVA)" was used to evaluate the Cutting speed v_c. The "Hierarchical Stepwise Selection" method was chosen to reduce insignificant predictors at the significance level of 0.05, i.e., an insignificant input factor was included in the model if its interaction or square was significant. The coefficient of determination $R^2 = 97.30\%$, which means that the model describes 97.30% of the variability in the measured response. Table 3 shows the outputs from the ANOVA. There are mainly relative increments of the variability of individual factors, interactions and their groups (Contribution column), the effects of these factors and interactions and p-value. p-value determines whether the factor is significant ($p < 0.05$) or insignificant ($p \geq 0.05$). It was not possible to test the adequacy of the model, because all repeated speed measurements at the central point came out the same, which is a pity from a statistical point of view, but from a technological point of view, it is perfect repeatability, which is very good.

Another output is the regression equation (Equation (1)) itself, describing the dependence of the Cutting speed on the machine setting parameters:

$$v_c = 3.772 - 0.202T_{on} - 0.009T_{off} - 0.026v - 0.012I - 0.001T_{off} \cdot T_{off} + 0.004T_{on} \cdot T_{off} + \\ +0.005T_{on} \cdot I + 0.001T_{off} \cdot I. \quad (1)$$

The last output is a graph of this dependence (Figure 2) for the two most important parameters Pulse on time and Discharge current. The remaining two parameters were fixed at the optimal level; see Section 3.5. Multicriteria optimization.

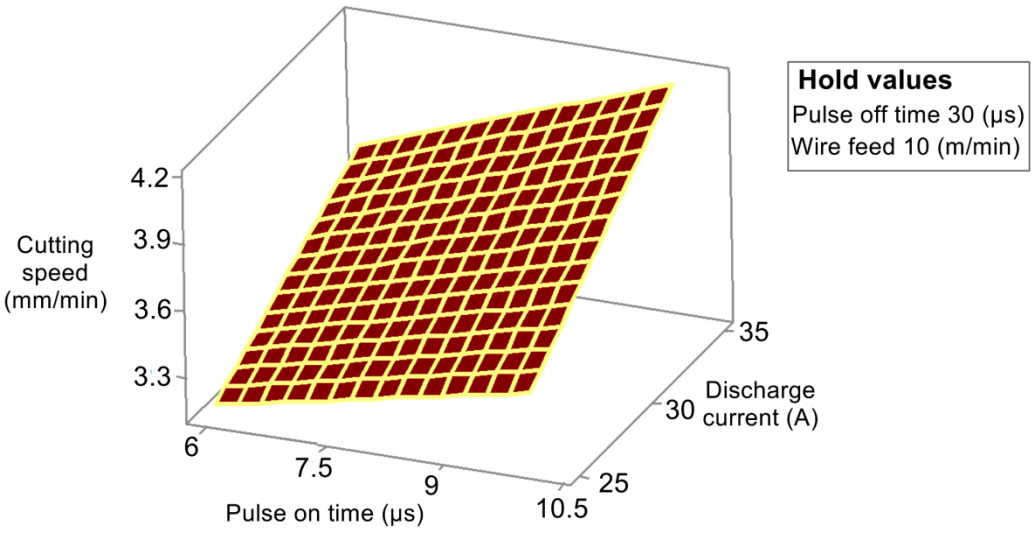

Figure 2. The response area showing the dependence of the Cutting speed on the two most important parameters.

3.3. Statistical Evaluation of Sample Surface Topography

The topography of the functional surface affects the service life and reliability of the component. The accuracy of the machine parts, their noise, the running-in time, friction losses, electrical resistance, heat transfer, wear resistance, etc., are dependent on the topography. The topography, therefore, affects the course of chemical and physical phenomena that accompany the operational activity of the functional surface of the part. The evaluation and use of the topography to increase the quality and thus the efficiency of machine parts aresome of the basic reasons for its detailed study. Therefore, in this experiment, two profile parameters and two of their surface equivalents were evaluated, namely arithmetical mean deviation of profile (Ra), maximum height of profile (Rz), arithmetical mean height (Sa) and maximum surface height (Sz). All topography parameters and 3D reliefs were evaluated using a contact 3D profilometer Dektak XT supplied by the manufacturer Bruker according to the corresponding standard for surface parameters ISO 25178-2 [23] and profile parameters ISO 4287 [24].

Five random places on each sample were selected for the measurement and then averaged from these values.

The topography parameters that were evaluated are compiled into clear graphs in Figure 3a, it is clear that the variance of the measured values between the individual samples is relatively significant, which confirms the dependence of the topography parameters on the setting of the machine parameters. If we talk about the most commonly used parameter of the topography Ra, its lowest value Ra = 2.85 μm was evaluated in Sample 20, which was machined with the parameters of the machine settings: U = 70 V, T_{on} = 6 μs, T_{off} = 50 μs, v = 14 m·min^{-1} and I = 25 A and its 3D relief is shown in Figure 4b. Although Bisaria [15] achieved lower Ra values when machining the same material, most of the sample's values were significantly higher than those of this study. However, the Ra value in the machining of this material was clearly reduced by using multicutin the Mandal studies [12,13]. From the comparison of 3D reliefs of the sample with the lowest value of Ra and Sample 1 with Ra = 3.03 μm, it is clear that the topography in the form of individual craters is not suitable for the assessment using only one parameter, but for complex assessment, it is necessary to evaluate more of their parameters.

A full quadratic regression model including "Analysis of Variance (ANOVA)" was used to evaluate Ra. The "Hierarchical Stepwise Selection" method was chosen to reduce insignificant predictors at the significance level of 0.05, as well as when modelling the Cutting speed, so insignificant input factors were included in the model if its interaction or quadratwas significant. The determination coefficient R^2 = 78.22%, which means that the model describes 78.22% of the variability in the measured response. Table 4 shows the outputs from ANOVA, relative increments of the variability of individual factors, interactions and their groups. The model was adequate, which means that it was without significant influence of other unmonitored factors, because p-Value$_{\text{Lack-of-Fit}} \geq 0.05$. Similar models would be achieved for other topography parameters.

Table 4. VarianceofRa.

Ra (μm)	Contribution	Effect	*p*-Value
Model	78.22%		0
Linear	61.84%		0
Gap voltage(V)	1.97%	0.0794	0.137
Pulse on time (μs)	29.81%	0.3092	0
Pulse offtime (μs)	0.95%	−0.0553	0.296
Discharge current(A)	29.11%	0.3056	0
2-Way Interaction	16.39%		0.001
Gap voltage(V)*Pulse offtime (μs)	6.49%	−0.1530	0.01
Pulse on time (μs)*Discharge current(A)	9.90%	0.1890	0.002
Error	21.78%		
Lack-of-Fit	19.93%		0.149
PureError	1.84%		
Total	100.00%		

* Multiplication symbol.

Regression Equation (2) describing the dependence of the topography parameter Ra on the machine setting parameters:

$$Ra = 1.919 + 0.034U - 0.206T_{on} + 0.043T_{off} - 0.045I - 0.0007U \cdot T_{off} + 0.009T_{on} \cdot I \quad (2)$$

The graph of this dependence for the two most important parameters Pulse on time and Discharge current is shown in Figure 3c, while the remaining two parameters were fixed at the optimal level,

see Section 3.5. Multicriteria Optimization. The curvature of the response surface caused by the Pulse on time*Discharge current interaction is clearly visible from the surface plot.

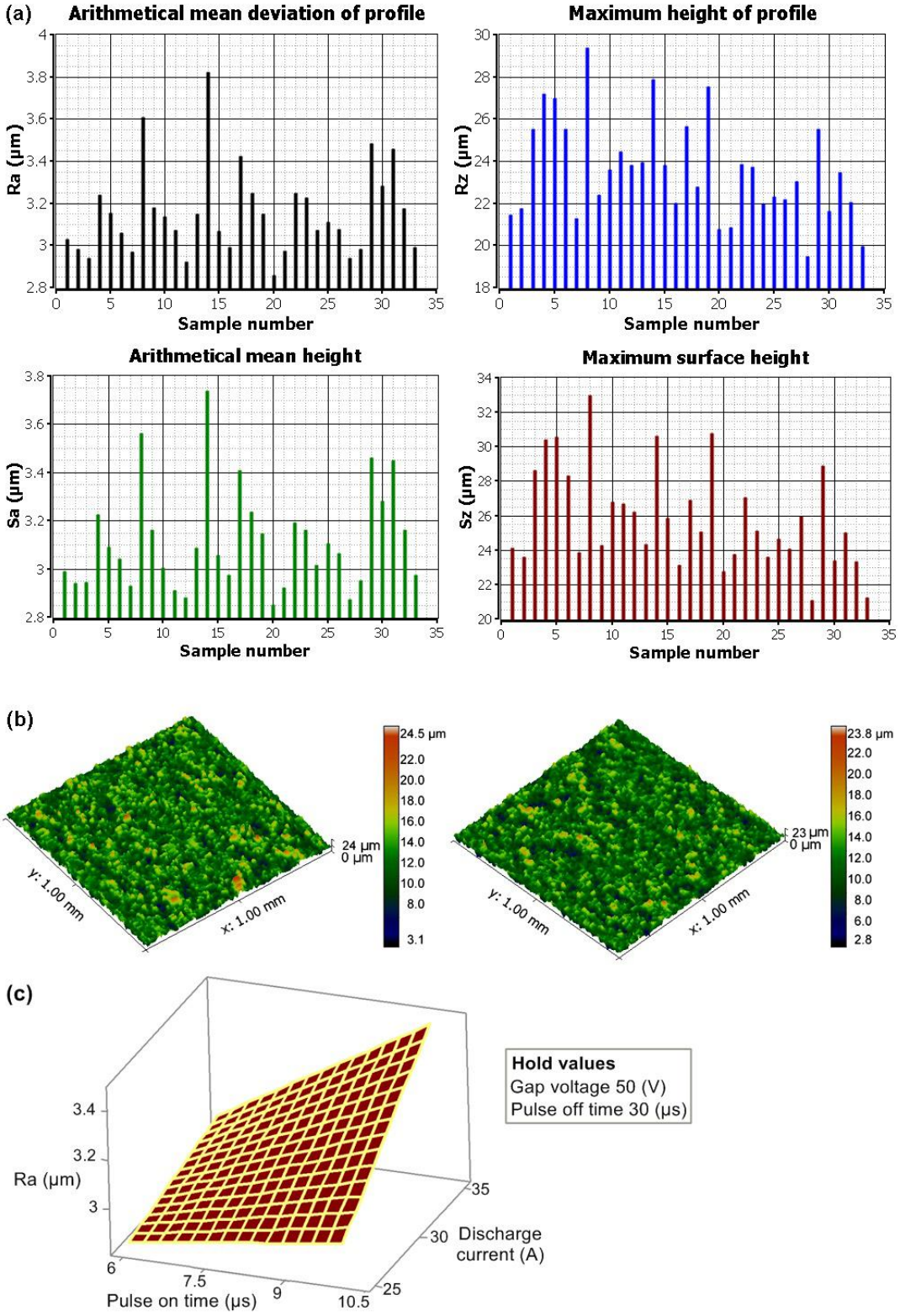

Figure 3. (**a**) The evaluated parameters Ra, Rz, Sa and Sz of individual experimental samples; (**b**) 3D reliefs of Samples 1 and 20; (**c**) the response area showing the dependence of Ra on the two most important parameters.

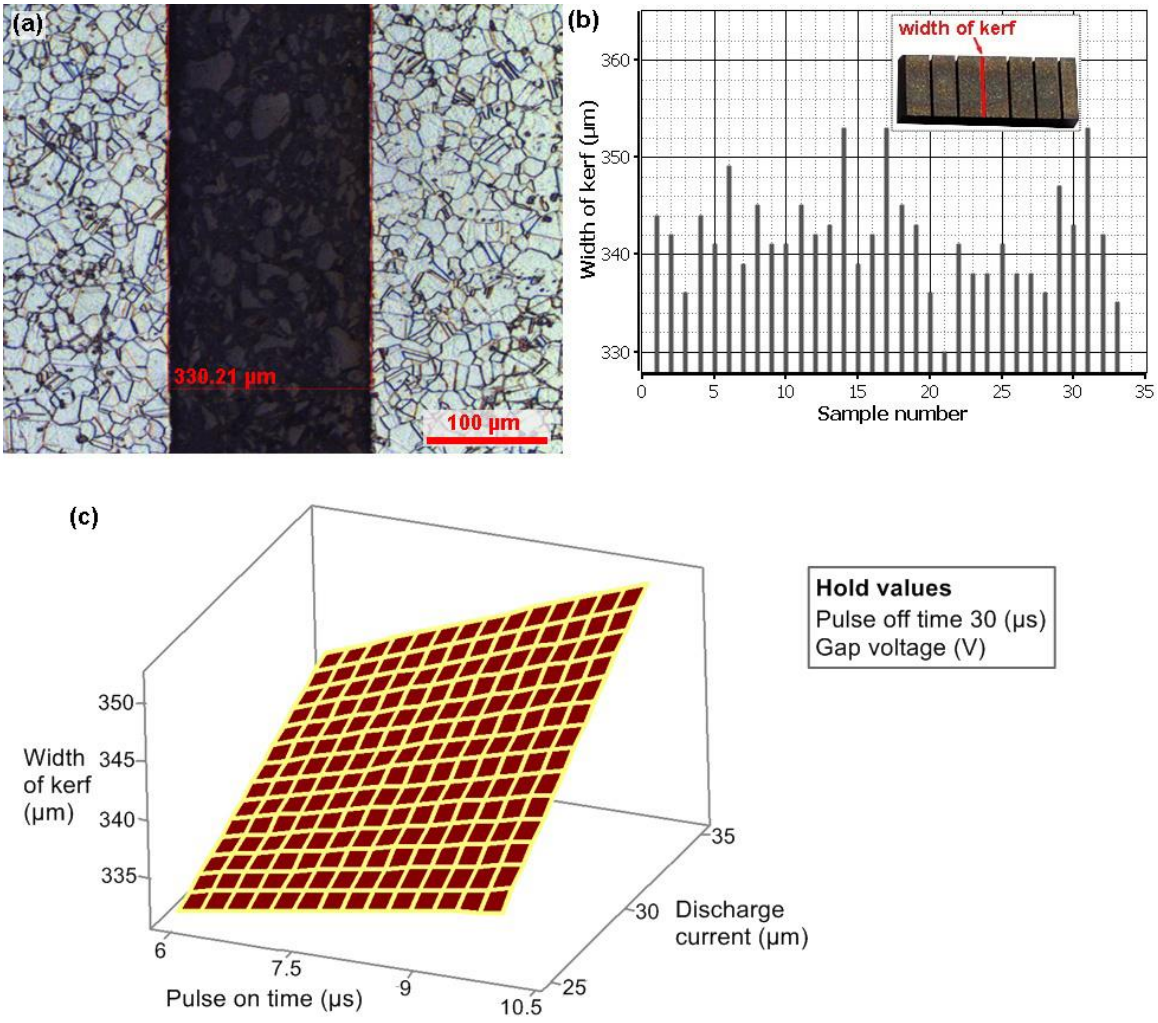

Figure 4. (**a**)Example of cut gap measurement, Sample 21; (**b**) the measured values of cut gaps for individual samples; (**c**) the response area showing the dependence of Width of kerf on the two most important parameters.

3.4. Statistical Evaluation of the Cutting Gap Affecting the Machining Accuracy

During the WEDM process, the eroded material also evaporates, resulting in the kerf w shown in Figure 4b. The size of this gap is directly dependent on the set of physical and mechanical properties of the machined material and also especially on the setting of machine parameters. Width of the kerf is a very important parameter that needs to be carefully monitored, as it affects the final dimension of the machined workpiece—its accuracy, as well as having a limiting effect on the production of the smallest possible radius of the inner radius, as presented in the Werner study [25]. The cut gaps, which were measured for individual samples (in cross-section—metallographic preparation) according to the principle shown in Figure 4a using a Zeiss light microscope were summarized in the graph in Figure 4b. It is clear from the graph that the lowest measured value of the width of the cut gap was in Sample 21 (machine setting parameters: U = 50 V, T_{on} = 6 µs, T_{off} = 30 µs, v = 14 m·min^{-1} and I = 25 A) and only 330 µm. Such a narrow cut gap is typical for the annealed steel 16MnCr5, which was investigated in the Mouralova study [26], which dealt with the evaluation of cut gaps for various materials and their additional heat treatments. For the Nimonic C 263 material, these cut gaps have never been examined, only for the Nimonic 80, while the width of the gaps according to the Goswami study [27] was similar.

The same regression and selection method was used to evaluate the gap was for the response in terms of the Cutting speed and surface topography. The model created for Width of kerf describes

85.28% of the variability in the measured response. The outputs from ANOVA are given in Table 5, which are mainly relative increments of the variability of individual factors, interactions and their groups. Then there are the effects of these factors and interactions and the *p*-value, which determines whether the factor is significant (*p*-Value < 0.05) or insignificant (*p*-Value ≥ 0.05). The model is adequate, which means that it is without any significant influence of other unmonitored factors, because $p\text{-Value}_{\text{Lack-of-Fit}} \geq 0.05$.

Table 5. VarianceofWidth of kerf.

Width of Kerf (μm)	Contribution	Effect	*p*-Value
Model	85.28%		0
Linear	75.47%		0
Gap voltage(V)	3.71%	2.667	0.017
Pulse on time (μs)	28.05%	7.333	0
Pulse offtime (μs)	0.41%	0.889	0.401
Discharge current(A)	43.30%	9.111	0
2-Way Interaction	9.81%		0.001
Pulse on time (μs)*Discharge current(A)	4.53%	3.125	0.009
Pulse offtime (μs)*Discharge current(A)	5.28%	−3.375	0.005
Error	14.72%		
Lack-of-Fit	12.30%		0.454
PureError	2.41%		
Total	100.00%		

* Multiplication symbol.

The Regression Equation (3) describing the dependence of the Width of kerf on the machine settings parameters is as follows:

$$w = 287.1 + 0.133U - 2.85T_{on} + 1.057T_{off} + 1.011I + 0.156T_{on} \cdot I - 0.033T_{off} \cdot I \quad (3)$$

Another output is a graph of this dependence for the two most important parameters, which are the same as for Cutting speed and the topography parameter Ra Pulse on time and Discharge current. The remaining two parameters were again fixed at the optimal level, which is described in more detail in the following Section 3.5. Multicriteria Optimization. This time, the Pulse on time*Discharge current interaction is less significant, and therefore the response area appears to be a plane, although, in reality, it is not.

3.5. Multicriteria Optimization

From the models in the previous three sections, it is clear that the input parameters Pulse on time and Discharge current always have the greatest influence on the responses. Both factors have a positive effect on all responses, which can be seen from the fact that the response areas are increasing for both factors. This property is also evident from the Main effects plot shown in Figure 5b, where it can be seen that the influence of these factors is greater than the others.

Unfortunately, we maximize the Cutting speed, but we minimize Ra and Width of the kerf, so the requirement for maximum speed goes against the requirement for minimum Ra and the requirement for minimum Width of kerf and creates a technical contradiction. In these cases, it is necessary to use multicriteria optimization; in our case, the Response Optimizer was used, which is a part of Minitab 17. The requirement for maximum speed and minimum Ra seemed to be the most significant; therefore, they were assigned twice as much importance. The graphical output was the Overlaid Contour Plot shown in Figure 5a, where the desired range of responses can be entered and their intersection is

indicated as a white area in the graph. Furthermore, the optimal settings of the machine are indicated here, which is part of the following text output.

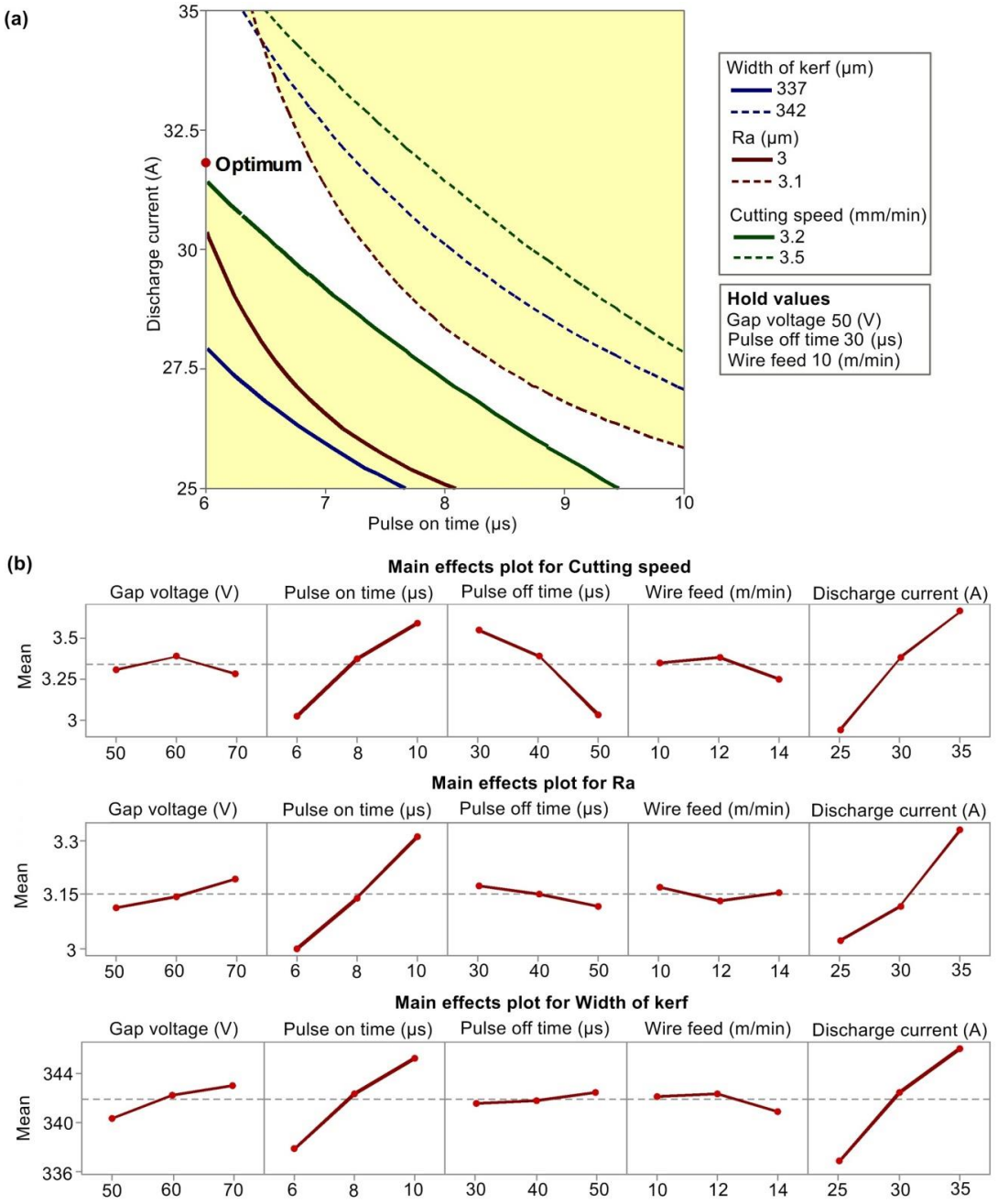

Figure 5. (**a**) Overlaid Contour Plot, (**b**) Main effects plot for Cutting speed, Ra and Width of the kerf.

The output of the procedure is the optimal setting of the machine parameters $U = 50$ V, $T_{on} = 6$ µs, $T_{off} = 30$ µs, $v = 10$ m·min^{-1} and $I = 31.67$ A, where the response values are given in Table 6 including 95% of confidence intervals for mean response values and 95% of prediction intervals for the individual value. A test sample was prepared for this setting and its values are listed in the Test column. These values fell into the prediction band, whereby we validated the model in the calculated optimal setting.

Table 6. Response values including 95% of prediction and confidence bands and test sample response value.

Response	Fit	95% CI	95% PI	Test
Width of kerf(μm)	338.02	(335.91; 340.14)	(333.01; 343.04)	341
Ra (μm)	2.9264	(2.8084; 3.0444)	(2.6715; 3.1814)	2.967
Cutting speed (mm/min)	3.4975	(3.4077; 3.5873)	(3.3117; 3.6833)	3.4

3.6. The Morphology of the Machined Surfaces, the Analysis of Chemical Composition and Subsurface Area

Wire electrical discharge machining is a thermoelectric process that removes the material from a workpiece (partial and tool electrodes) and creates a specific morphology formed by several craters on it. These craters, arising after individual periodically recurring electric discharges, are of various shapes, depending on the set of mechanical and physical properties of the machined material (including the type of heat treatment) and the setting of the machine parameters. The eroded material is washed away in the form of small balls by a stream of dielectric liquid; however, sometimes these balls also stick to the machined surfaces. Another factor that contributes to the loss of workpiece material is its evaporation due to very high process temperatures, which are in the range of 10,000–20,000 °C [28]. These temperatures also cause massive diffusion processes between the wire electrode and the material being machined. The material near the surface in the order of micrometres is completely melted, being cooled rapidly due to the immediate cooling effect of the dielectric liquid. The layer modified in this way is called the recast layer and was studied on almost all machined materials but in different local amounts of occurrence. The surface morphology and possible defects are key parameters determining the final quality of the machined surface, allowing the prediction of the correct functionality of the part and its service life.

The study of the surface morphology of all machined samples was performed using electron microscopy. In all cases, a secondary electron detector SE was used for imaging, while the samples were always studied at a magnification of 1000×, 2500× and then 4000×.

The morphology of all machined samples in the planned experiment looked similar, so Figures 6 and 7 show the morphology of Sample 20 (machined by setting the machine parameters: U = 70 V, T_{on} = 6 μs, T_{off} = 50 μs, v =14 m·min^{-1} and I =25 A), which had the lowest value of the topography parameter Ra and only 2.85 μm and this was examined in more detail. From Figure 7, it is apparent that the surface is covered with a relatively large amount of recast layer containing the placeswith mixed copper from the wire electrode. There was a significantly smaller amount of zinc from the electrode, only 2.3 wt.%. This difference is due to the different solubility of copper and zinc in the machined material. Copper is present in the base material only in 0.07 wt.% and zinc is not present here at all. The diffusion phenomenon was also studied in the Bisaria study [15]; however, it was absolutely minimal compared to the results in this study. However, this could be due to a different EDX measurement method, in which Bisariaanalysed the side of the workpiece in the recast layer area and not the entire area of the machined surface as in this study. However, in both studies, the same conclusion was reached in terms of the occurrence of cracks, where they were not found on any of the machined samples.

The analysis of the chemical composition at the individual characteristic places on the workpiece surface was shown in Figure 7. It is clear that areas that are smooth and not covered by the recast layer contain significantly less diffused copper from the wire electrode and no zinc. They are also covered with almost half the amount of oxygen, which shows a lower degree of oxidation of such a surface.

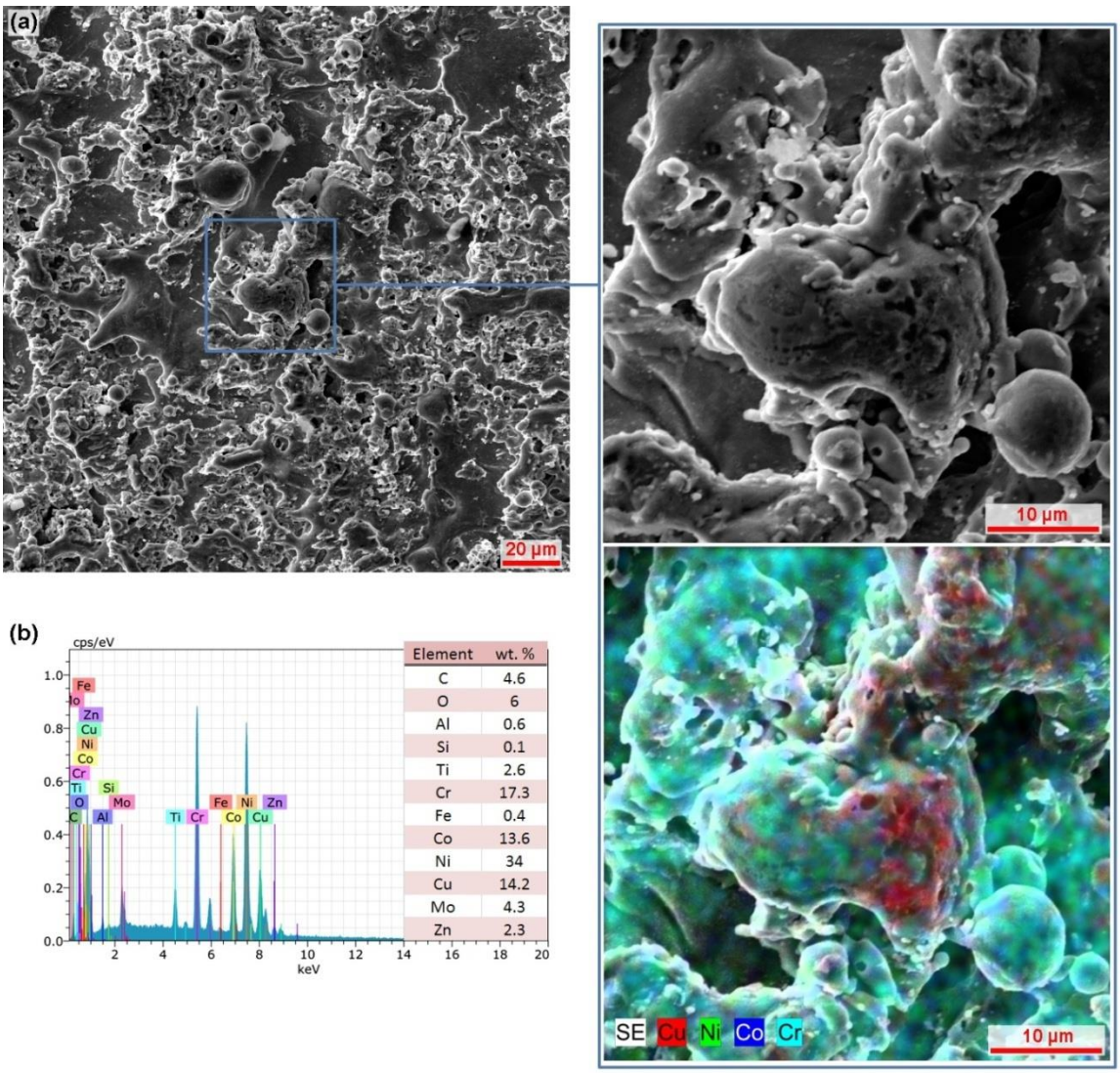

Figure 6. The surface morphology of Sample 20 (SEM/SE) and the analysis of chemical composition: (**a**) the morphology of the sample including the detail and its analysis of the distribution of Cu, Co and Cr elements; (**b**) the spectrum of the chemical composition in the area shown in (**a**) and the number of individual elements contained here.

The analysis of the subsurface layer was performed on pre-prepared metallographic preparations of all samples using electron microscopy. This analysis is crucial because in many materials, extensive defects in the form of cracks or burnt cavities have been found in this way, e.g., in the Mouralova study [6,7,10], that significantly affect the correct and required functionality of the component and its service life during subsequent use. The cross-sections were observed on a Lyra3 device using a backscattered electron (BSE) detector, each with a magnification of 1000× and then 2500× and 4000×.

From Figure 8a–d it is clear that the samples produced have a similar appearance of the subsurface area and the thickness of the recast layer is at most 20 µm thick. The recast layer is not continuous, but very jagged, as indicated by the view from the topin Figure 6. None of the produced samples has subsurface defects in the form of burnt cavities or cracks, which is very favourable in terms of the required functionality and durability of parts machined in this way. Given similar studies such as Goswami [11,17], Bisaria [15] or Sonawane [16], it can be said that Nimonic material does not tend to form subsurface cracks after WEDM, which is a very positive fact.

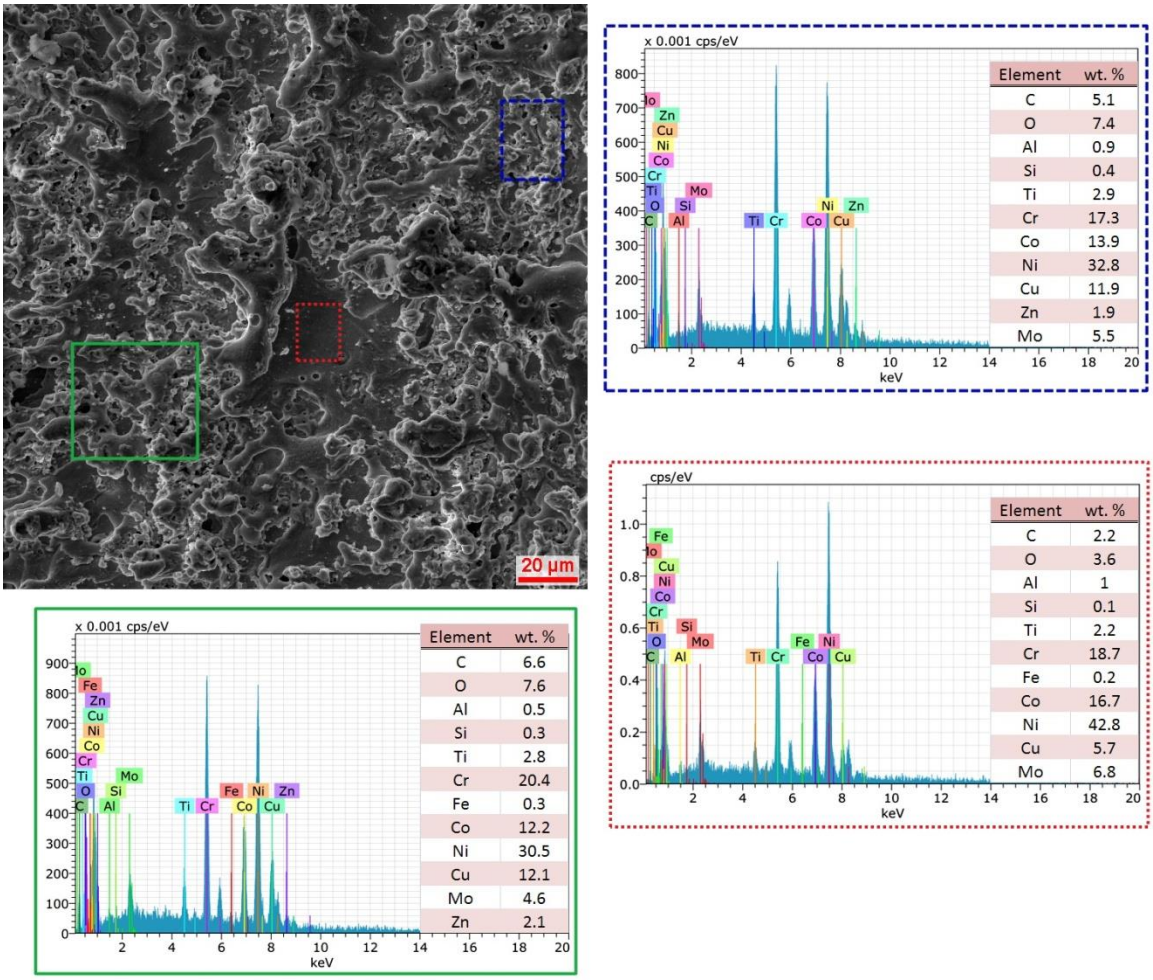

Figure 7. The surface morphology of Sample 20 (SEM/SE) and the analysis of chemical composition in individual areas.

3.7. TEM Lamella Analysis

The lamella made using a focused intense beam on a Helios electron microscope from Sample 20 was analysed in a Titan transmission electron microscope. During the measurement, the so-called scanning mode (STEM) with an accelerating voltage of 300 kV and a current in the beam of 1 nA was used to ensure the optimal strength of the detected X-rays by the EDX detector. Only elements with a significant local change in concentration are shown in the element maps in Figure 9 in individual EDX measurements. The elements with a concentration lower than 1% or even distribution on the sample (e.g., copper for EDX 2) are listed only in Table 6. From Figure 9, where the lamellae produced is shown, it is clear that the upper cover layer was made of carbon, while the concentration of chromium, copper and titanium in the area of the recast layer also increased. Furthermore, interesting round particles composed mainly of titanium were found. The exact chemical composition of the individual examined details 1–4is summarized in Table 7. The increased amount of copper in the sample compared to the standardized composition of Nimononic C 263 is probably due to the re-deposition of the material during the sputtering or migration of the material from the tool brass electrode. From a chemical point of view, it is clear from the detail of EDX 2 that in the lower part of the lamella the distribution of the elements is constant, except for the re-presence of a titanium particle. From EDX 3 the local change in the concentration of individual elements in the upper part of the lamella near the recast layer can be seen in more detail. Thus, the concentration of titanium, chromium, copper, nickel, cobalt and, to a lesser extent, sulphur increased in the investigated area. In addition, an increased amount of zinc was

detected for the first time, indicating that some of the copper contamination came from the migration of material from the wire electrode. A similar effect of electrode material migration was reported by the Singh group [29]. Due to the presence of interesting titanium particles, additional EDX 4 measurements were performed to determine the exact chemical composition of this detail. The detailed measurements of titanium particles showed that they are predominantly composed of titanium, with a small proportion of chromium and aluminium. In addition to the chemical composition, the effect of WEDM on the crystal lattice of the material was also investigated. For this purpose, a diffraction mode with a total beam current of 8 nA was used. The size of the beam trace during the measurement was about 200 nm. From a comparison of the individual points shown in the diffraction patterns in Figure 9, it can be seen that there was a slight change in position, indicating residual stress. The formation of residual stress on the Nimonic surface after WEDM machining was also observed by XRD group of Bisaria [15]. In addition, other diffraction spots appeared, indicating the formation of other crystal planes in the study area.

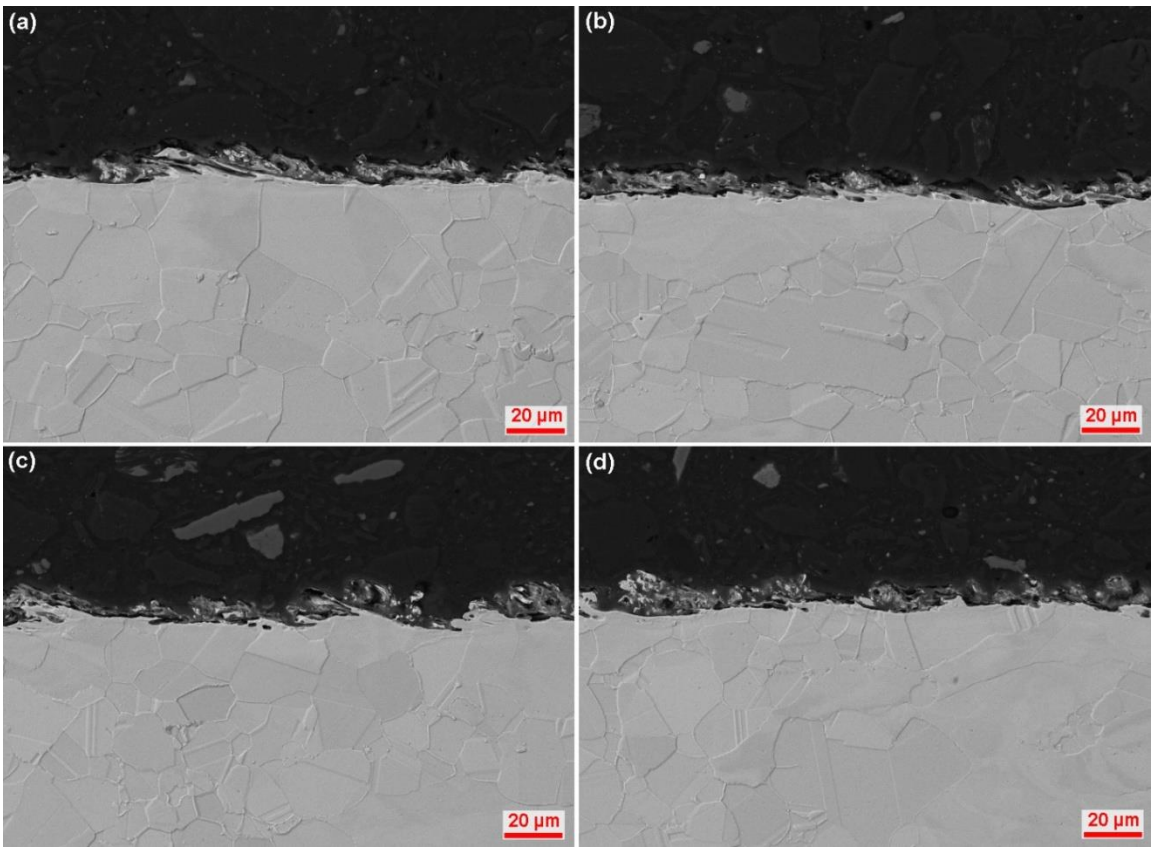

Figure 8. The cross-sections of the SEM/BSE samples: (**a**) Sample 1 machined by setting the machine parameters: U = 70 V, T_{on} = 8 µs, T_{off} = 40 µs, v = 12 m·min^{-1} and I = 30 A; (**b**) Sample 10 machined by setting the machine parameters: U = 60 V, T_{on} = 8 µs, T_{off} = 40 µs, v = 14 m·min^{-1} and I = 30 A; (**c**) Sample 20 machined by setting the machine parameters: U = 70 V, T_{on} = 6 µs, T_{off} = 50 µs, v = 14 m·min^{-1} and I = 25 A; (**d**) Sample 30 machined by setting machine parameters: U = 70 V, T_{on} = 6 µs, T_{off} = 30 µs, v = 14 m·min^{-1} and I = 35 A.

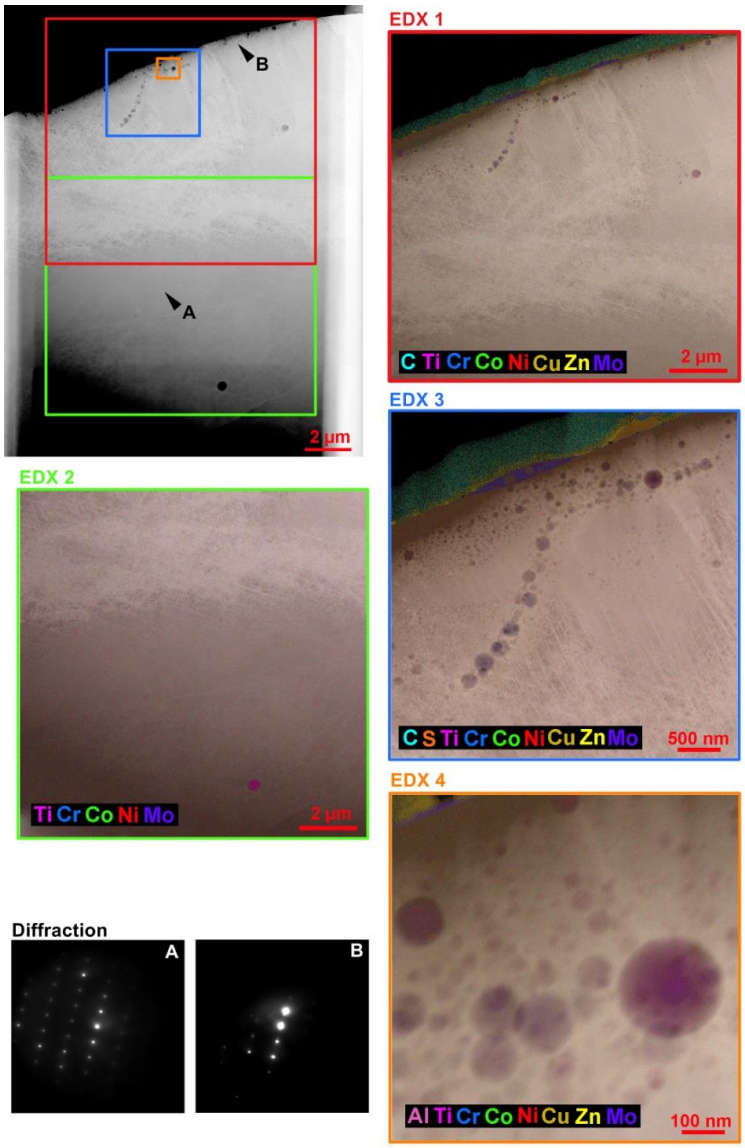

Figure 9. TEM lamella including the maps of the distribution of individual elements in various details and diffraction patterns.

Table 7. Composition in individual details of EDX according to Figure 9.

	EDX 1		EDX 2		EDX 3		EDX 4	
Element	**Atomic Fraction (%)**	**Atomic Error (%)**	**Atomic Fraction (%)**	**Atomic Error (%)**	**Atomic Fraction (%)**	**Atomic Error (%)**	**Atomic Fraction (%)**	**Atomic Error (%)**
S	0.26	0.07	0.17	0.06	0.33	0.11	0.17	0.09
C	0.06	0.02	1.37	0.33	0.70	0.17	1.24	0.29
Ti	2.30	0.43	2.32	0.43	2.29	0.42	4.28	0.76
Cr	22.23	4.12	21.71	4.02	21.78	4.01	19.86	3.60
Co	18.04	3.35	17.57	3.25	17.73	3.26	16.37	2.92
Ni	47.70	8.85	47.00	8.70	46.72	8.61	42.07	7.59
Cu	5.16	0.96	4.64	0.86	6.26	1.15	9.83	1.75
Zn	0.00	0.00	0.00	0.00	0.30	0.06	0.96	0.17
Mo	3.20	0.58	3.04	0.55	3.29	0.59	3.27	0.57
Al	0.39	0.09	0.66	0.16	0.46	0.11	1.09	0.25
B	0.00	0.06	0.91	0.17	0.00	0.09	0.00	0.16
Si	0.13	0.03	0.33	0.08	0.15	0.03	0.38	0.09
Fe	0.50	0.09	0.28	0.05	0.26	0.05	0.48	0.09
Mn	0.03	0.01	0.00	0.00	0.00	0.01	0.00	0.00

4. Conclusions

The subject of the research of this study was optimization enabling precise machining of the Nimonic C 263 super alloy using wire electrical discharge machining technology. The following conclusions were reached by performing a designof experiments of 33 rounds, in which five input factors were systematically changed in the form of the machine parameters Pulse off time, Gap voltage, Discharge current, Pulse on time and Wire feed:

- the highest Cutting speed was achieved for Sample 14, namely 4.1 mm·min^{-1} with the setting of machine parameters: U = 70 V, T_{on} = 10 µs, T_{off} = 30 µs, v = 10 m·min^{-1} and I = 35 A, and it was found that the factors Pulse on time and Discharge current influence this response the most;
- the topography analysis showed that the lowest values of the parameter Ra = 2.85 µm were achieved in Sample 20, which was machined with the following machine settings: U = 70 V, T_{on} = 6 µs, T_{off} = 50 µs, v = 14 m·min^{-1} and I = 25 A, while Pulse on time and Discharge current were also the factors most influencing the response;
- the cut gap that most affects machining accuracy was the smallest for Sample 21 machined with machine setting parameters: U = 50 V, T_{on} = 6 µs, T_{off} = 30 µs, v = 14 m·min^{-1} and I = 25 A, at only 330 µm;
- regression equations were created describing the dependence of the Cutting speed, Width of kerf and surface topography parameter Ra on machine setting parameters,
- using multicriteria optimization, it was found and verified by testing that with the requirement of maximizing Cutting speed, and simultaneous minimization of Ra and Width of the kerf is the optimal setting of machine parameters: U = 50 V, T_{on} = 6 µs, T_{off} = 30 µs, v = 10 m·min^{-1} and I = 31.67 A;
- the morphology analysis showed the absence of any surface or subsurface defects in the form of cracks or burnt cavities in all machined samples, with the recast layer moving to a maximum thickness of 20 µm;
- the EDX analysis showed significant diffusion processes between the wire electrode and the workpiece, with 15 wt.% of Cu and about 2 wt.% of Zn adhering to the surface of the sample;
- the analysis of the produced TEM lamella showed in detail its composition at the atomic level, including clear maps of individual elements, diffraction patterns in the area of the recast layer and the base material were also displayed.

Based on the above-mentioned conclusions, it can be clearly stated that with the help of complex optimization tools, it is possible to significantly streamline the machining of Nimonic C 263 super alloy and achieve both financial savings in the form of reduced machine time and increased quality of machined surfaces.

Author Contributions: Conceptualization, K.M. and R.Z.; methodology, K.M., T.P. and J.B.; validation, K.M., Z.F., J.F. and L.B.; formal analysis, Z.F. and R.Z.; investigation, K.M., R.Z., T.P., Z.F. and J.F.; resources, K.M. and L.B.; data curation, K.M., J.B. and T.P.; writing—original draft preparation, K.M.; writing—review and editing, K.M..; supervision, K.M.; funding acquisition, L.B., Z.F. and J.F. All authors have read and agreed to the published version of the manuscript.

Funding: CzechNanoLab project LM2018110 funded by MEYS CR is gratefully acknowledged for the financial support of the measurements/sample fabrication at CEITEC Nano Research Infrastructure. This work was supported through the internal grant provided by the Jan Evangelista Purkyně University in Ústí nad Labem, called SGS (Student Grant Competition), No. 0004/2015, and partly by the Ministry of Education, Youth and Sport of the Czech Republic, the program NPU1, project No. LO1207.This work was supported by the Brno University of Technology Specific Research Program, project no. FSI-S-17-4464.

Acknowledgments: This research work was technically supported by Intemac Solutions, Ltd., Kurim.

Conflicts of Interest: The authors declare no conflict of interest.

References

1. Vates, U.K. *Wire-EDM Process Parameters and Optimization*; Springer: Berlin/Heidelberg, Germany, 2018; ISBN 978-620-2-30578-5.
2. Jahan, M.P. *Electrical Discharge Machining (EDM): Types, Technologies and Applications*; Nova Science Publishers: Hauppauge, NY, USA, 2014.
3. Kibria, G.; Jahan, M.P.; Bhattacharyya, B. *Micro-Electrical Discharge Machining Processes*; Springer: Singapore, 2019; ISBN 978-981-13-3074-2.
4. Gowthaman, P.S.; Jeyakumar, S. A Review on machining of High Temperature Aeronautics Super-alloys using WEDM. *Mater. Today Proc.* **2019**, *18*, 4782–4791. [CrossRef]
5. Koyilada, B.; Gangopadhyay, S.; Thakur, A. Comparative evaluation of machinability characteristics of Nimonic C-263 using CVD and PVD coated tools. *Measurement* **2016**, *85*, 152–163. [CrossRef]
6. Mouralova, K.; Prokes, T.; Benes, L.; Sliwkova, P. Analysis of subsurface defects occurrence in abrasion resistant Creusabro steel after WEDM including the study of morphology and surface topography. *Mach. Sci. Technol.* **2019**, *24*, 274–290. [CrossRef]
7. Mouralova, K.; Prokes, T.; Benes, L.; Bednar, J. The Influence of WEDM Parameters Setup on the Occurrence of Defects When Machining Hardox 400 Steel. *Materials* **2019**, *12*, 3758. [CrossRef]
8. Mouralova, K.; Benes, L.; Bednar, J.; Zahradnicek, R.; Prokes, T.; Matousek, R.; Hrabec, P.; Fiserova, Z.; Otoupalik, J. Using a DoE for a comprehensive analysis of the surface quality and cutting speed in WED-machined hadfield steel. *J. Mech. Sci. Technol.* **2019**, *33*, 2371–2386. [CrossRef]
9. Mouralova, K.; Benes, L.; Zahradnicek, R.; Bednar, J.; Hrabec, P.; Prokes, T.; Matousek, R.; Fiala, Z. Quality of surface and subsurface layers after WEDM aluminum alloy 7475-T7351 including analysis of TEM lamella. *Int. J. Adv. Manuf. Technol.* **2018**, *99*, 2309–2326. [CrossRef]
10. Mouralova, K.; Prokes, T.; Benes, L. Surface and subsurface layers defects analysis after WEDM affecting the subsequent lifetime of produced components. *Arabian J. Sci. Eng.* **2019**, *44*, 7723–7735. [CrossRef]
11. Goswami, A.; Kumar, J. Investigation of surface integrity, material removal rate and wire wear ratio for WEDM of Nimonic 80A alloy using GRA and Taguchi method. *Eng. Sci. Technol. Int. J.* **2014**, *17*, 173–184. [CrossRef]
12. Mandal, A.; Dixit, A.R.; Das, A.K.; Mandal, N. Modeling and optimization of machining nimonic C-263 superalloy using multicut strategy in WEDM. *Mater. Manuf. Process.* **2016**, *31*, 860–868. [CrossRef]
13. Mandal, A.; Dixit, A.R.; Chattopadhyaya, S.; Paramanik, A.; Hloch, S.; Królczyk, G. Improvement of surface integrity of Nimonic C 263 super alloy produced by WEDM through various post-processing techniques. *Int. J. Adv. Manuf. Technol.* **2017**, *93*, 433–443. [CrossRef]
14. Amitesh, G.; Jatinder, K. An investigation into the machining characteristics of nimonic 80A using CNC wire-EDM. *Int. J. Adv. Eng. Technol.* **2012**, *3*, 170–174.
15. Bisaria, H.; Shandilya, P. Experimental investigation on wire electric discharge machining (WEDM) of Nimonic C-263 superalloy. *Mater. Manuf. Process.* **2019**, *34*, 83–92. [CrossRef]
16. Sonawane, S.A.; Kulkarni, M.L. Optimization of machining parameters of WEDM for Nimonic-75 alloy using principal component analysis integrated with Taguchi method. *J. King Sauduniv. Eng. Sci.* **2018**, *30*, 250–258. [CrossRef]
17. Goswami, A.; Kumar, J. Optimization in wire-cut EDM of Nimonic-80A using Taguchi's approach and utility concept. *Eng. Sci. Technol. Int. J.* **2014**, *17*, 236–246. [CrossRef]
18. Kumar, V.; Jangra, K.K.; Kumar, V.; Sharma, N. WEDM of nickel based aerospace alloy: Optimization of process parameters and modelling. *Int. J. Interact. Des. Manuf. (IJIDeM)* **2017**, *11*, 917–929. [CrossRef]
19. Singh, B.; Misra, J.P. Empirical modelling of wear ratio during WEDM of nimonic 263. *Mater. Today Proc.* **2018**, *5*, 23612–23618. [CrossRef]
20. Ezilarasan, C.; Velayudham, A. Effect of machining parameters on surface integrity in machining Nimonic C-263 super alloy using whisker-reinforced ceramic insert. *J. Mater. Eng. Perform.* **2013**, *22*, 1619–1628. [CrossRef]
21. Mouralova, K. Moderní Technologie Drátového Elektroerozivního Řezání Kovových Slitin. Ph.D. Thesis, Brno University of Technology, Brno, Czech Republic, 2015.
22. Montgomery, D.C. *Design and Analysis of Experiments*; John Wiley & Sons: Hoboken, NJ, USA, 2017; ISBN 9781119113478.

23. ISO25178-2. *Geometrical Product Specifications (GPS)—Surface Texture: Areal-Part 2: Terms, Definitions and Surface Texture Parameters*; International Organization for Standardization: Geneva, Switzerland, 2012.
24. ISO 4287. *Geometrical Product Specifications (GPS)-Surface Texture: Profile Method—Terms, Definitions and Surface Texture Parameters*; International Organization for Standardization: Geneva, Switzerland, 1997.
25. Werner, A. Method for enhanced accuracy in machining curvilinear profiles on wire-cut electrical discharge machines. *Precis. Eng.* **2016**, *44*, 75–80. [CrossRef]
26. Mouralova, K.; Kovar, J.; Klakurkova, L.; Prokes, T. Effect of Width of Kerf on Machining Accuracy and Subsurface Layer After WEDM. *J. Mater. Eng. Perform.* **2018**, *27*, 1908–1916. [CrossRef]
27. Goswami, A.; Kumar, J. Surface topography and Kerf study of Nimonic 80A using Wire-cut EDM. *Mater. Sci. Forum* **2015**, *808*, 35–41. [CrossRef]
28. McGeough, J.A. *Advanced Methods of Machining*; Springer Science & Business Media: Berlin, Germany, 1988.
29. Singh, B.; Misra, J.P. Empirical modeling of cutting speed during WEDM of nimonic 263. *J. Phys. Conf. Ser.* **2019**, *1240*, 012035. [CrossRef]